

Convective and Diffusive Energetic Particles Losses Induced by Shear Alfvén Waves in the ASDEX Upgrade Tokamak

M. García-Muñoz¹, N. Hicks¹, R. van Voornveld², I.G.J. Classen^{1,2}, R. Bilato¹, V. Bobkov¹, M. Bruedgam¹, H.-U. Fahrbach¹, V. Igochine¹, S. Äkäslompolo³, P. Lauber¹, M. Maraschek¹, K. Sassenberg¹, M. Schneller¹ and the ASDEX Upgrade Team

¹Max-Planck-Institut für Plasmaphysik, EURATOM Association

Boltzmannstr. 2, D-85748 Garching, Germany

²FOM-Institute for Plasma Physics Rijnhuizen, Association EURATOM-FOM,

PO Box 1207, 3430 BE Nieuwegein, The Netherlands

³Helsinki Univ. of Technology, Association Euratom-Tekes, P.O.Box 4100, FIN-02015 HUT, Finland

Future burning plasma experiments such as ITER may be subject to the excitation of Alfvén eigenmode (AE) instabilities by 3.5 MeV fusion born alpha particles as well as fast-ions created by auxiliary heating systems critical for current drive, heating, and momentum input. If allowed to grow unabated, these instabilities have the potential to cause fast-ion redistribution and loss leading to a degradation of the heating and current drive efficiencies as well as to possible serious damage of first wall components. Recently, in ASDEX Upgrade, significant progress has been achieved towards a better understanding of the fast-ion transport across magnetic field lines in the presence of multiple AEs. In ICRF heated plasmas, strong fast-ion losses in the presence of Alfvén Cascades (ACs) and Toroidal Alfvén Eigenmodes (TAEs) have been observed with a scintillator based Fast-Ion Loss Detector (FILD) [1]. Fluctuations in the electron temperature profile caused by the ACs and TAEs have been measured with the ECE radiometer at high resolution in space (≈ 1 cm) and time (1 MHz sampling rate). Fig.1 shows the normalized cross power spectral

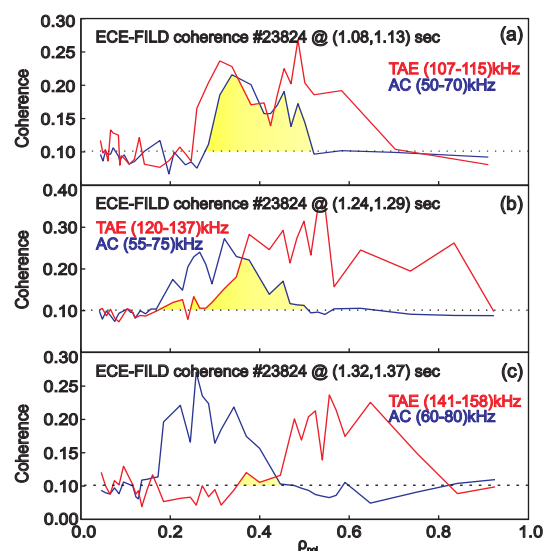


Figure 1: AUG discharge #23824: ACs and TAEs radial structures. Different time intervals are displayed; (a) for (1.08-1.13) sec, (b) for (1.24-1.29) sec and (c) for (1.32, 1.37) sec. In yellow, overlapping ranges of TAE-AC internal structures well before the AC-TAE transition are highlighted.

(≈ 1 cm) and time (1 MHz sampling rate). Fig.1 shows the normalized cross power spectral

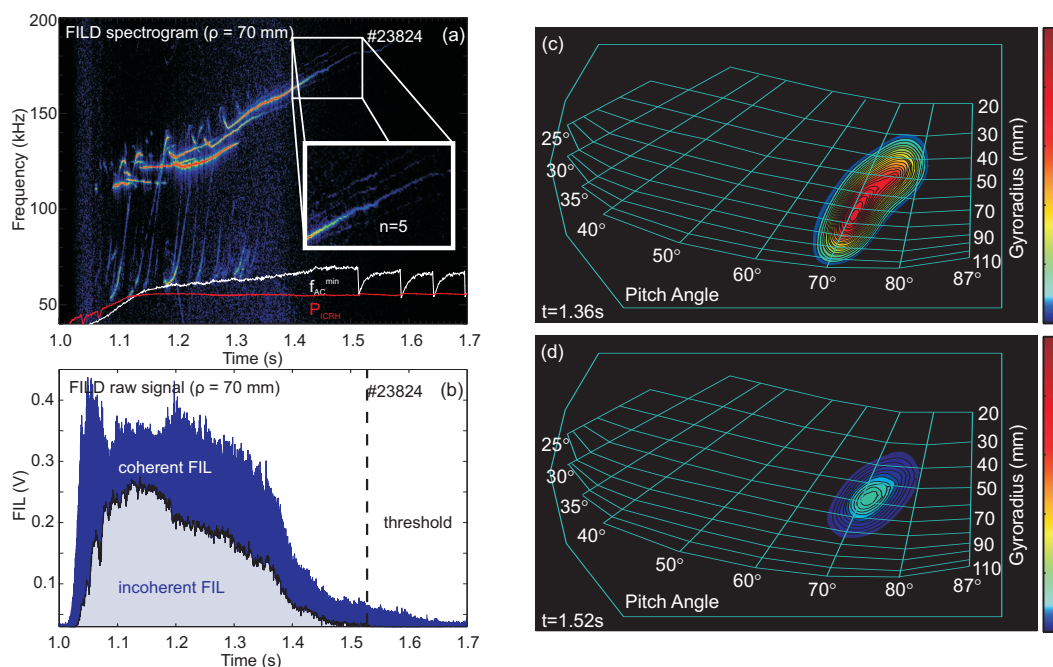


Figure 2: AUG discharge #23824: (a) spectrogram of the fast-ion loss signal with gyroradius ≈ 70 mm. The lowest AC frequency, f_{AC}^{min} , is superimposed in white while the total ICRH power (P_{ICRH}) is superimposed in red. (b) Fast-ion loss signal. The coherent and incoherent components of the losses are highlighted. The vertical dashed line depicts the threshold for the incoherent losses. (c) Phase-space of fast-ion losses at $t=1.36$ s, and at $t=1.52$ s (d).

densities (coherence) as a function of ρ_{pol} and frequency for 50 ms time intervals. The AC and TAE radial structures were obtained by selecting and averaging a certain frequency band of the coherence. The selected AC and TAE frequency bands are given in Fig.1. As Fig.1 shows, their overlapping region (highlighted in yellow) becomes smaller with time. A detailed analysis of the time-resolved fast-ion losses detected with the FILD system during the AE activity allows to identify the loss mechanisms [2]. Fig. 2(a) shows the coherent fast-ion losses due to ACs and TAEs. The raw data of the Fourier-analyzed fast-ion loss signal shown in Fig. 2(a) are presented in Fig. 2(b) to investigate the diffusive and convective character of the losses. The signal consists of a modulated (coherent) signal sitting on an incoherent background whose amplitude varies with time. The coherent component of the fast-ion losses is correlated in frequency and phase with the corresponding magnetic fluctuation, yielding to the spectrogram shown in Fig. 2(a). The incoherent component is dominant, up to 80% of the total losses, in the presence of multiple frequency chirping AEs, $t \approx (1.1-1.3)$ s, and decreases when the number of modes decreases. However, it should be noted that it is not zero when only one mode is ejecting ions if its amplitude is large enough, $t \approx (1.42-1.52)$ s. During the time window $t \approx (1.52-1.7)$ s only coherent

losses induced by a single TAE, $n = 5$, are visible. Going backwards in time, the incoherent losses appear, for $t \leq 1.52$ s, when the local maximum radial displacement of the magnetic field lines is larger than ≈ 2 mm as measured by its fluctuation induced on the SXR emission. This threshold in the fluctuation amplitude is indicated in Fig. 2(b) with a vertical dashed line.

In order to fully characterize the orbits of the lost ions and identify the wave-particle resonances responsible for the losses, the phase-space (energy and pitch angle) of the fast-ion losses is shown in Fig. 2-(c) and -(d). In the presence of multiple AEs, e.g., $t = 1.36$ s, fast ions are ejected within a broad energy range with a gyroradius from $\rho \approx 35$ mm up to $\rho \approx 105$ mm, see Fig. 2(c). For the magnetic field at the probe, $Bt \approx 1.6$ T, this gyroradius range corresponds to hydrogen ions with energies between $E = 0.2$ and $E = 1.4$ MeV. As expected from ICRH heated plasmas the fast-ion losses appear at high pitch angles between 67° and 80° . The phase space of lost fast ions changes strongly during the evolution of the AE activity, showing a completely different pattern within the next 200 ms. Fig.2(d) presents fast-ion losses well localized at high pitch angles ($\approx 71^\circ$) and energies ($\rho \approx 60$ mm). The basic properties of the coherent and incoherent losses are investigated through their dependence on the magnetic fluctuation amplitude. Tracking the frequencies of the individual fluctuations in both, magnetics and FILD spectrograms, we get the relationship between the coherent fast-ion losses and the corresponding magnetic fluctuation amplitude. Fig.3(a) shows the results for the TAE $n=3$ between $t=1.24$ s and $t=1.32$ s. A clear linear dependence is visible during the whole time window, showing the convective character of the underlying loss mechanism. A similar analysis has been done for the incoherent losses shown in Fig.2(b). The envelope of the incoherent losses, black curve in Fig.2(b), is plotted in Fig.3(b) as a function of the amplitude of the TAE $n=5$ for a time interval close to the onset of the incoherent losses, insert in Fig.3(b), $t=(1.42,1.50)$ s. A clear quadratic dependence has been obtained, strongly suggesting a diffusive mechanism involving several reso-

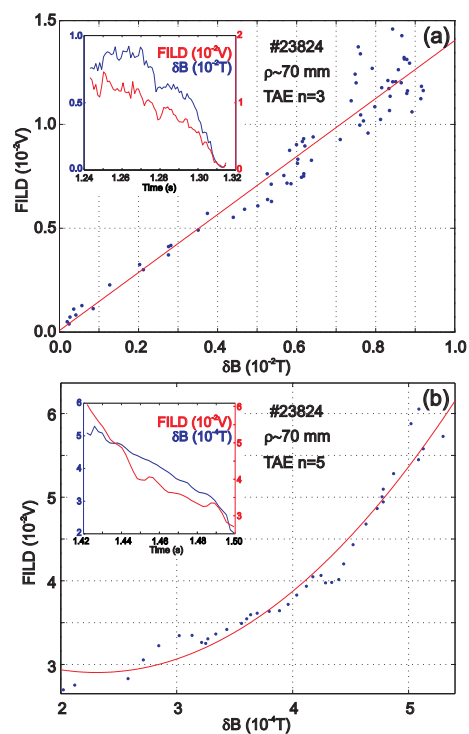


Figure 3: AUG discharge #23824: Fast-ion loss rate. (a) Linear dependence of the coherent losses at the TAE $n=3$ frequency on the MHD fluctuation amplitude. (b) Quadratic dependence of the incoherent losses on the TAE $n=5$ fluctuation amplitude.

nances in phase-space. This is supported by the data shown in Fig.2(c) which indicates that the losses cover a larger domain in phase-space when the incoherent signal is not zero. It should also be underlined that, as shown in Fig.2(b), the incoherent component is even larger in the presence of several modes, which is also expected to induce a diffusive fast-ion transport.

Simulations with the full orbit code GOURDON and the guiding center drift orbit code HAGIS have been performed to better understand the nature of the escaping ions and their interactions with the AE waves. The possible wave-particle resonances fulfilled by the fast-ion orbital poloidal (ω_θ) and toroidal (ω_ϕ) frequencies and AE frequencies (ω) are studied using an extended version of the HAGIS code including fields in the vacuum region outside of the separatrix. A wave-particle exchange of momentum, P , and energy, E , takes place if the resonant condition $\Omega_{n,p} = n\omega_\phi - p\omega_\theta - \omega \approx 0$ is fulfilled. By plotting, $\log(1/\Omega_{n,p})$ in the energy range of the fast-ions measured by FILD, we can identify the regions of phase space where a resonant interaction could occur [3,4]. Fig.5 shows all possible wave-particle resonances with TAEs $n=3$ and 4 and ACs $n=3, 5$ and 7 at their lowest frequency. With the whole fast-ion phase-space covered by resonances, virtually all ions can interact resonantly with the AE waves, enabling the fast-ion transport in phase-space through orbit stochasticity. While single resonant interactions lead to rapid convective losses, the overlapping of multiple resonances and mode radial structures may be responsible for the strong diffusive losses observed in the experiments presented here. Stochastic fast-ion losses due to multiple Alfvén/acoustic modes may be of concern in large fusion devices such as ITER.

References

- [1] M. Garcia-Munoz et al., Rev. Sci. Instrum. **80**, 053503 (2009)
- [2] M. Garcia-Munoz et al., Phys. Rev. Lett. **104**, 185002 (2010)
- [3] S. D. Pinches et al., Nucl. Fusion **46**, S904 (2006)
- [4] M. Garcia-Munoz et al., Nucl. Fusion **49**, 085014 (2009)

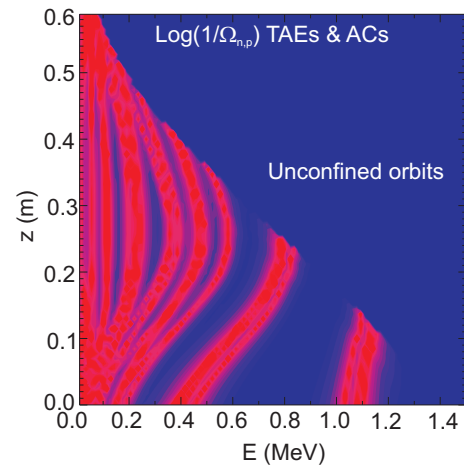


Figure 4: AUG discharge #23824: phase-space resonance lines between the on-axis ICRF heated hydrogen ions and the $n = 3$, $n = 5$ and $n = 7$ ACs and the $n=3$ and $n=4$ TAEs.